Catalysis Science & Technology

Accepted Manuscript

This article can be cited before page numbers have been issued, to do this please use: D. Huth and M. Rose, *Catal. Sci. Technol.*, 2021, DOI: 10.1039/D0CY02434A.

ROYAL SOCIETY OF CHEMISTRY

rsc.li/catalysis

View Article Online
DOI: 10.1039/D0CY02434A

Catalysis Science & Technology

ARTICLE

Selective catalytic synthesis of short chain oxymethylene ethers by a heteropoly acid – a reaction parameter and kinetic study

Received 00th January 20xx,
Accepted 00th January 20xx

DOI: 10.1039/x0xx00000x

www.rsc.org/

Daniel Huth[a], and Marcus Rose*[a]

Oxymethylene ethers (OME) are considered as low-emission additive or replacement to diesel fuel. They can be synthesized by different routes based on C_1 platform chemicals in different oxidation states. The challenge is to tune the acidic catalyst for the condensation reaction to a selectivity for a certain oligomeric fraction (OME_{3-5}) for optimal fuel properties. Herein, we report the use of heteropoly acids that showed an outstanding activity and selectivity for the production of the respective OME fraction under very mild reaction conditions. Trioxane and dimethoxymethane (OME_1) were used as substrates which are both products of the methanol value-added chain. Reaction parameters such as catalyst/substrate ratio and temperature could be reduced considerably due to a high catalytic activity and selectvity. Kinetic data were obtained experimentally and modelled to estimate the reaction rate, activation energy and pre-exponential factor as a solid basis for further reaction engineering.

Introduction

In recent years synthetic fuels have attracted increasing attention beyond first generation biofuels as additive to fossil gasoline and diesel as they show certain benefits in production and application. On the one hand, their production from non-fossil resources and renewable energy has emerged as a sustainable alternative in concepts such as Biomass-to-Liquid (BtL)[1] and Power-to-X (P2X).[2] On the other hand, combustion properties can be improved by reduction of soot and NO_X emissions that are typically inversely proportional. [3, 4] Combustion in oxygen excess decreases soot formation while NO_x is increased due to higher combustion temperatures. In contrast, lowering the combustion temperature reduces NO_x but increases soot formation due to incomplete combustion of the hydrocarbons. This trade-off can be overcome by using oxygenated fuels or fuel additives. In recent years oxymethylene ethers (OME) or poly(oxymethylene) dimethyl ethers have contributed to significant advances in the field. [3, 5-9] OME are oligomeric ether-based hydrocarbons with the following molecular formula: CH_3-O-(CH_2-O-)$_n$-CH_3. Their physicochemical properties vary with the chain length n. The shortest, OME_0, is dimethyl ether, followed by OME_1, also known as methylal or dimethoxymethane (DMM). OME_1 and OME_2 can be used as an additive which lowers the pollutant emission significantly.[4] To hit the pure diesel specification OME_{3-5} are suitable.[10] $OME_{>5}$ shows also good properties, but they are under normal conditions solid.

OME can be produced by different routes. Recently, a direct synthesis of OME_1 from syngas was reported for the first time using impregnated Ru/γ-Al_2O_3 such as molecular Ru and Co catalysts. [11, 12] Even before, the hydrogenation of CO using Ru–Ni/Al_2O_3 as catalyst was reported to yield formaldehyde as a hemiacetal-stabilized form with methanol and water.[13] In contrast, the more established routes start from different C_1 bulk chemicals with syngas-based methanol at the beginning of the value-added chain and formaldehyde (FA) with its various derivatives such as trioxane as reactants.[14] While the initial reaction step typically yields OME_1 as intermediate the subsequent chain growth occurs by addition of formaldehyde units. While the initial reaction step is a condensation reaction that is thermodynamically limited due to the water formation[15] the chain growth reaction occurs without the formation of water and hence, is not prone to the limitations of the equilibrium reaction involving water.[16] In the presence of water also several side reactions occur yielding OME derivatives with different terminal groups such as hemi-formals and glycols. For an industrial process the substrate would be preferentially methanol and formaldehyde as the most common platform chemicals for the formation of OME_1 with a subsequent step to chain growth by reaction with formaldehyde or its derivatives.[17] All routes have been reported in literature and in all cases acidic catalysts are required. Various kinds of molecular and solid acids, such as metal oxides (WO_3), mineralic acids (e.g. sulphuric acid) and acidic ion exchange resins have been investigated.[18-20] Recently, Fink et al. showed based on zeolites that a moderately strong acidity is required.[21] Wang et al. and Burger et al. used acidic ion exchange resins and zeolites under batch reaction conditions to obtain the

[a] Technical University of Darmstadt, Ernst-Berl-Institut für Technische und Makromolekulare Chemie, Alarich-Weiss-Straße 8, 64287 Darmstadt
* Corresponding author: rose@tc2.tu-darmstadt.de
† Footnotes relating to the title and/or authors should appear here.
Electronic Supplementary Information (ESI) available: [details of any supplementary information available should be included here]. See DOI: 10.1039/x0xx00000x

preferred OME_{3-5} fraction from trioxane (TRI) as formaldehyde source and starting from DMM. [5, 22, 23] DMM-trioxane-Ratios (DTR) about 2, high catalyst ratios, temperatures up to 90 °C and reaction times of more than 20 minutes resulted in conversions >90% and a selectivity <30% for OME_{3-5}. Both groups found ion exchange resins to be superior to zeolites. Lautenschütz et al. chose more mild reaction parameters using an ion exchange resin.[24] With 40 °C at atmospheric pressure and a fifth of the catalyst amount used in the other studies and also with a DTR of 2 gives comparable results in more than the twice the reaction time. Overall, most of all OME studies focus on conventional zeolites and ion exchange resins as commercially available catalysts. To the best of our knowledge so far the use of heteropoly acids has not been investigated although attracted high attention in catalysis and other applications.[25, 26] They have only been mentioned as potential catalysts in patent applications but apparently not investigated at all.[27, 28] Hence, in this study we report for the first time the use of heteropoly acids as catalysts for the formation of OME from DMM and trioxane as model reaction.[29] Based on a catalyst and reaction parameter screening a detailed kinetic study was carried out to prove the excellent catalytic performance of HPA in OME formation.

Results and discussion

Screening of solid acid catalysts

Based on previous reports typical solid acid catalysts were screened initially for the OME formation (Scheme 1) starting from DMM and trioxane (Table 1). The reactions were carried out at a temperature of 60 °C at autogenous pressure of 3.1 bar in a batch stainless steel pressure reactor. For the initial screening a DTR of 2 was applied according to the previous studies for reasons of comparison. 5 wt-% of the respective solid acid catalyst regarding the total mass of both substrates was added. Samples were taken after a reaction time of 5 h and quantified by gas chromatography (GC).

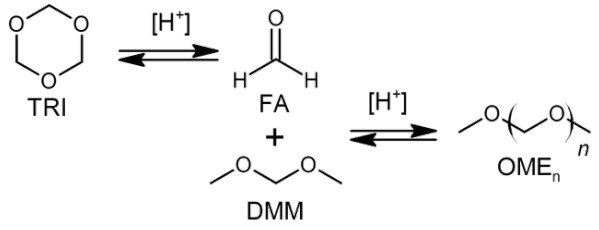

Scheme 1. Formation of OME from DMM and trioxane as model reaction for the kinetic investigation.

The screening of commercially available acidic zeolites (ZSM5 and HBEA25) and an ion exchange resin (Purolite CT175DR), a sulfonated macroporous polystyrene/divinylbenzene resin that is typically applied for the catalytic production of methyl *tert*-butyl ether (MTBE) exhibited results comparable to the previously reported studies. [5, 23, 24] Less conventional solid acids based on tungsten oxides such as tungstic acid (H_2WO_4) and pure tungsten oxide (WO_3) showed only neglible to no catalytic activity. Additionally, two commercial acidic alumina catalysts Puralox® SCCA from Sasol were tested. Only moderate trioxane conversions of up to 48 % with OME_{3-5} yields of 29 % are obtained.

Table 1. Selectivity and yield of OME_{3-5} and trioxane conversion of all solid acid catalysts in the initial screening. Reactions were carried out in a stainless steel reactor for 5 hours at 60 °C, 3.1 bar, stirrer speed 1000 min^{-1} and a DTR of 2.

Solid acid		$S(OME_{3-5})$	$Y(OME_{3-5})$	X(trioxane)
ZSM5		0.509	0.506	0.941
HBEA25		0.459	0.387	0.929
Purolite CT175DR		0.512	0.517	0.927
tungstic acid (H_2WO_4)		0.000	0.000	0.000
tungsten(VI) oxide (WO_3)		0.000	0.000	0.004
Puralox	SCCa-5/200 W8	0.436	0.294	0.481
	SCCa-5/200 P4	0.265	0.011	0.028
phosphotungstic acid ($H_3PW_{12}O_{40}$)		**0.525**	**0.573**	**0.928**

In contrast, phosphotungstic acid ($H_3PW_{12}O_{40}$) a well-known and investigated heteropoly acid[25] exhibited high trioxane conversions of 93 % with OME_{3-5} yields of 57 %. At first glance, the activity seems to be in a similar order of magnitude as for the tested zeolites and ion exchange resins. However, in contrast to these catalysts the final reaction mixture of the phosphotungstic acid contains a considerable amount of a white solid product. The results displayed in Table 1 are based on the liquid phase GC analysis which is able to quantify the products up to OME_8. The occurring solid products are higher oligomers and maybe even polymeric species ($OME_{>>6}$) that are not soluble anymore in the reaction mixture that contains the lower liquid OME as a major fraction. Hence, it can be concluded that phosphotungstic acid is a catalyst with an unexpected high activity compared to the other conventionally applied solid acid catalysts. Maybe the formation of solid products is the reason that there are no reports on the formation of the lower OME using phosphotungstic acid as catalyst, yet.

Due to the promising results reaction parameters were varied to identify more mild conditions that prevent the formation of higher OME that might precipitate. The DTR was kept constant while the reaction temperature and the amount of catalyst was drastically reduced to 30 °C and 0.2 wt-% of catalyst, respectively. Also, the reaction was carried out in a glass round bottom flask at ambient pressure avoiding evaporation of the low boiling components by a condenser and enabling a more convenient sampling during the course of the reaction. The catalyst was added when the reaction mixture was thermally stable at 30 °C. Due to the high activity of the catalyst, the exothermicity of the reaction (Δh_R=-25.2 kJ mol^{-1})[15] in this setup and a low temperature level an unavoidable temperature rise of up to 38 °C 2 min after catalyst addition was observed. Already after 5 minutes a trioxane conversion of more than 93 % was observed.

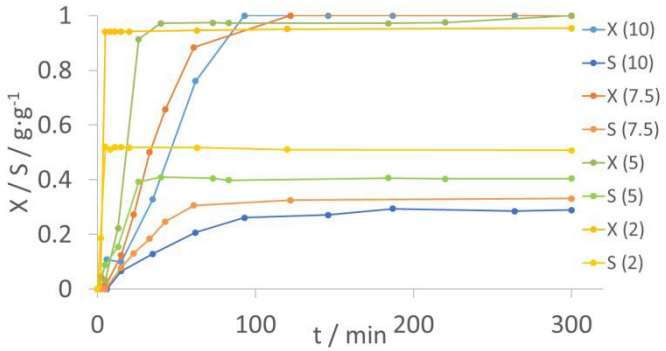

Figure 1: Trioxane conversions and selectivites of OME_{3-5} at varying DTR (value in brackets). All other parameters are constant (30 °C, 1 atm, 0.2 wt-% catalyst). The measured points are connected by straight dashed lines for clarity only.

Influence of concentration and temperature

In order to find a suitable window of reaction parameters the concentration, especially the DTR, as well as the influence of the temperature was investigated by measuring accurate concentration time profiles. The amount of trioxane as limiting reactant predominately determines the reaction rate (Figure 1). The rate increases with a decreasing DTR, i.e., an increasing trioxane amount. Connected to that, also the selectivity for the formation of OME_{3-5} increases. Increasing the DTR from 2 to 10 the reaction time to achieve a conversion >90 % increases from 5 min to >90 min with the OME_{3-5} selectivity decreasing from ca. 50 % to <30 %. The limiting factor is the amount of formaldehyde formed by the acid-catalysed decomposition of trioxane which is apparently the slowest and thus, limiting reaction in this system. If there are no or only very small amounts of trioxane in the reaction mixture the overall reaction rate decreases significantly. Also, the major by-product is actually the intermediate OME_2. Especially in the case of a higher DTR it is plausible as the amount of available formaldehyde is lower and hence, a further chain growth to the OME_{3-5} fraction is prevented. However, the OME_2 can be further transformed into the higher OME fraction by additionally adjusting reaction conditions or subsequent addition of TRI.

The reaction conditions investigated in this work avoid additional solvents. Due to the low boiling temperature (42 °C) and high vapour pressure of DMM the reaction at atmospheric pressure is limited to low temperatures. Hence, the temperature dependence is investigated at 25 °C, 30 °C and 40 °C (Figure 2). In order to obtain plausible and accurate kinetic data a higher DTR was chosen to allow sufficient temporal resolution by sampling at a lower reaction rate. Under these conditions also the exothermicity of the reaction is not an issue and the reaction can be carried out under isothermal conditions. As expected, the reaction rate increases with temperature. A conversion of >98 % is obtained after about 60 and 100 min at 40 and 30 °C, respectively. At 25 °C even after three hours a conversion of trioxane of less than 90 % at is observed. The selectivity for the formation of OME_{3-5} is about 25 % and depends only on the DTR as shown before

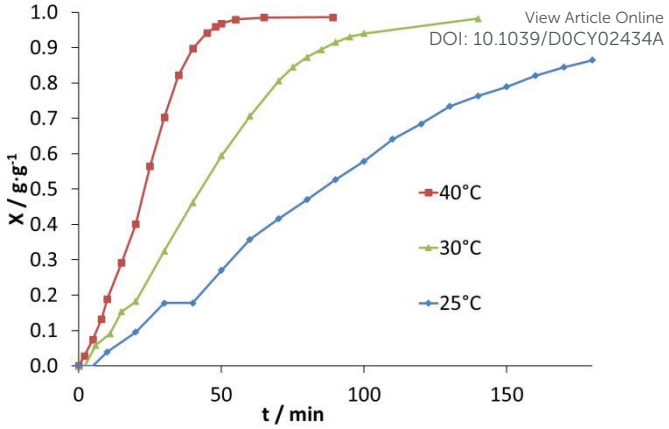

Figure 2. Trioxane conversions at 25 °C, 30 °C and 40 °C. All other parameters are constant (DTR 10, 1 atm, 0.2 wt-% catalyst, connecting lines are only added for clarity).

while the major product fraction is OME_2. The selectivity is not measurably influenced by the reaction temperature.

Reaction kinetics

The reaction kinetics of the formation of the lower OME fractions were determined by modelling the experimental time-resolved data at different reaction temperatures by parameter estimation using the software PRESTO-KINETICS®.[30] A power law kinetic model was applied based on the general reaction in scheme 2 to describe the chain growth of OME by addition of FA units by an equilibrium reaction.

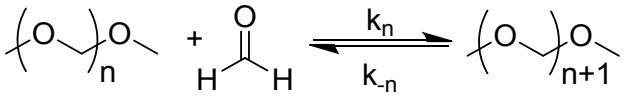

Scheme 2. Formation of OME_{n+1} from OME_n and FA as equilibrium reaction.

The addition of one formaldehyde building block to an OME_n forms OME_{n+1}. For the initial model this reaction is assumed to be an equilibrium reaction. Its rate is supposed to depend on the temperature-dependent reaction rate constant k_n. Since an equilibrium reaction is assumed, the reverse reaction is characterized by the rate constant k_{-n}. Formally, it is assumed that the trioxane equals three formaldehyde molecules. The equilibrium reaction to form formaldehyde from trioxane in DMM solution is not considered in the model due to the slower reaction compared to the OME formation reaction.[31] This is emphasized by the fact that FA cannot be detected as intermediate as it is directly converted to OME in the faster subsequent chain growth reaction. Hence, the kinetic model considers only the conversion of trioxane although being aware of the fact that the slower trioxane decomposition reaction might be the reaction limiting step. The differential equations for the first order kinetic model with respect to $c(OME_n)$ and c(1/3TRI) are described as follows:

$$r_n = \frac{dc(OME_n)}{dt} = -k_n(T)c(OME_n)c\left(\frac{TRI}{3}\right) + k_{-n}(T)c(OME_{n+1}) + k_{n-1}(T)c(OME_{n-1})c(TRI/3)$$

$$r_{1/3TRI} = \frac{dc(1/3TRI)}{dt} = \sum_{i=1}^{6}[-k_i(T)c(OME_i)c(TRI/3) + k_{-i}(T)c(OME_{i+1})]$$

The kinetic model considers the formation of OME of up to n=6 with the respective rate equation resulting in six differential equations for the OME_n concentration. Also, the trioxane concentration representing the limiting species and not considering the slow initial reaction step towards the FA formation is considered in the differential equation. Overall, this consists of twelve terms, for each equilibrium reaction of the considered OME_n. Consequently, the overall reaction network model consists of seven interdependent differential equations. The equations are solved numerically by means of the implicit Crank-Nicolson method. To estimate the k_n and k_{-n} values the software PRESTO KINETICS® was used. The obtained values are shown in Table 2.

Table 2. Temperature-dependent reaction rate constants determined by modelling the experimental data with the software PRESTO-KINETICS® for parameter estimation.

k_n	Unit	25 °C	30 °C	40 °C
k_1	L min^{-1} mol^{-1}	6.58E-04	1.34E-03	4.58E-03
k_{-1}	min^{-1}	1.26E-06	4.28E-09	8.38E-08
k_2	L min^{-1} mol^{-1}	1.60E-03	3.08E-03	9.00E-03
k_{-2}	min^{-1}	3.25E-08	4.27E-09	4.00E-12
k_3	L min^{-1} mol^{-1}	3.06E-03	6.05E-03	1.51E-02
k_{-3}	min^{-1}	3.76E-05	1.00E-04	1.42E-14
k_4	L min^{-1} mol^{-1}	3.65E-03	7.50E-03	1.78E-02
k_{-4}	min^{-1}	6.71E-06	2.84E-09	3.13E-07
k_5	L min^{-1} mol^{-1}	4.50E-03	9.50E-03	2.30E-02
k_{-5}	min^{-1}	1.00E-10	5.00E-03	2.83E-08
k_6	L min^{-1} mol^{-1}	0.00E+00	0.00E+00	0.00E+00
k_{-6}	min^{-1}	0.00E+00	0.00E+00	0.00E+00

As can be seen from the values in Table 2 all k_{-n} values for the reverse reaction to an OME_n of shorter chain length, are smaller by some orders of magnitude than the forward reactions (k_n) and thus, have little influence on the reaction course. As no OME_7 is formed at these conditions the k_6 and k_{-6} value is negligible. Regarding the residual function of the numerical solution using *PRESTO KINETICS®* these are the best fitting parameters. Nevertheless, the rate constants for backward reactions are prone to a certain error and could also be neglected in the kinetic model. Because of that, the reactions are not in a thermodynamic equilibrium, full conversion of trioxane is reached during the kinetic experiments which is the limiting factor and determines the final product composition of oligomeric OME fractions. In Figure 3 to 5 the measured concentration time profiles and the fitted reaction network model are shown. For the temperatures of 25 °C and 30 °C, the model fits well with the measured values. At a reaction temperature of 40 °C a pronounced deviation of experiment and model in the initial reaction phase is observed. The model appears to be faster than the measured values. This is most likely an artefact of the limiting substrate trioxane and its intermediate substrate formaldehyde. In the reaction model, the pre-equilibrium of the formaldehyde formation from trioxane is not taken into account as at low temperatures no formaldehyde is observed. The formaldehyde concentration is assumed to be three times the amount of trioxane based on the stoichiometric decomposition only within the model.

It was shown before by Giefer[32] and Walker[31] that the applied acid catalyst and its concentration, solvent and the temperature have an effect on the rate of trioxane equilibration with formaldehyde. Hence, at an increasing temperature this reaction becomes of greater importance and should be included in kinetic models at higher temperatures.

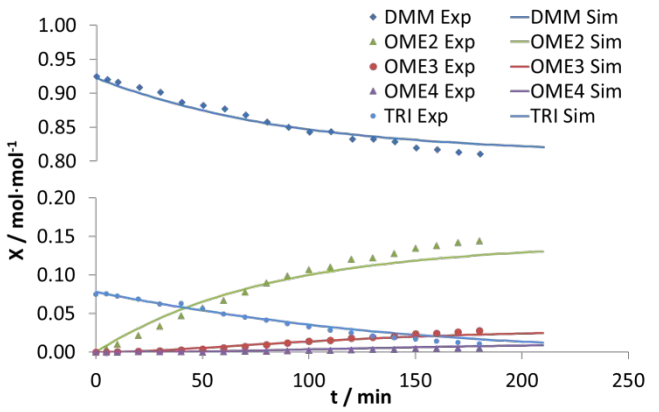

Figure 3. Experimental (points) and modelled (lines) concentration time profiles of both substrates and the major products at 25 °C.

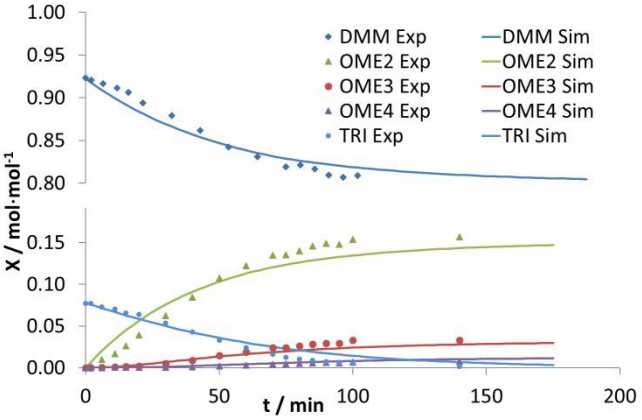

Figure 4. Experimental (points) and modelled (lines) concentration time profiles of both substrates and the major products at 30 °C.

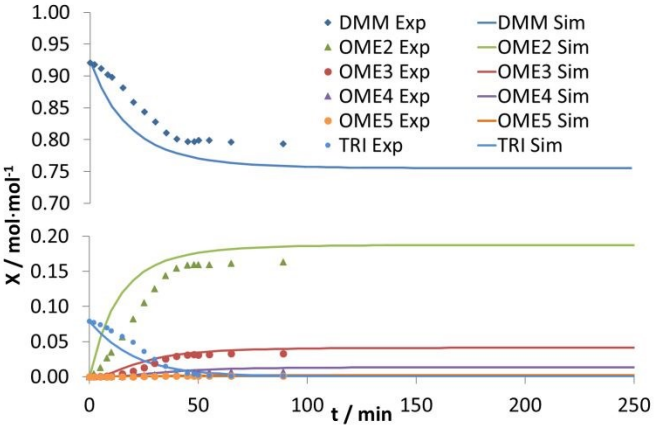

Figure 5. Experimental (points) and modelled (lines) concentration time profiles of both substrates and the major products at 40 °C.

Additionally, it is assumed that the reaction of trioxane to FA is much slower than the reaction of FA to an OME_n which would be the definition of the rate limiting step. So there is a low amount of

FA in the reaction solution. This challenge is also described by Walker.[31] The ratio of the reaction rate constants for the OME_n formation and the decomposition of trioxane at 40 °C seem not as high as it is for 25 °C and 30 °C. At lower temperatures this does not seem to have that much influence. Another reason for the deviation is that the model is kept rather simple in the form of a classical chain growth reaction.

The initial formation of FA can be considered the rate limiting step for the first two chain growth reactions to form OME_2 and OME_3. For these reactions the rate constants increase while for higher OME fractions the rate constants remain rather constant. This points towards the fact, that k_1 and k_2 have to be considered as effective rate constants that do not exclusively describe the microkinetic of the OME chain growth but are rather limited by the availability of FA and hence, by the kinetics of the decomposition reaction to provide FA as reactant. As the rate constants for the growth of OME_{4+} are rather constant it can be assumed that due to the low concentrations of the respective starting OME_{3+} the availability of FA is not the limiting factor anymore and the rate constants can represent the microkinetics of the chain growth without limitation by the initial decomposition reaction.

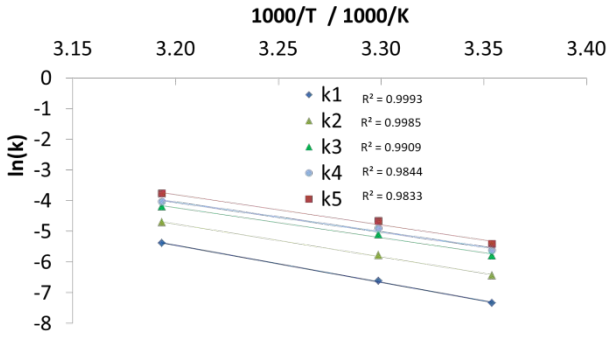

Figure 6. Arrhenius plot of estimated reaction rates, k_1 to k_5, each determined at three reaction temperatures.

Table 3. Slope (m) and axis intercept (n) out of the Arrhenius-plot and the calculated activation energies (E_a) and pre-exponential factors(k_0) for the individual oligomerisation reactions.

	m	n	E_a / *kJ·mol^{-1}*	k(0) / *L·mol^{-1}·min^{-1}*
k_1	-12022	33.016	99.96	2.2E+14
k_2	-10664	29.356	88.67	5.6E+12
k_3	-9761.6	27.007	81.16	5.4E+11
k_4	-9644.7	26.809	80.19	4.4E+11
k_5	-9922.4	27.955	82.50	1.4E+12

From the Arrhenius plot of k_1-k_5 (Figure 6) the activation energies and the pre-exponential factors for the OME chain growth reactions were determined (Table 3). The Arrhenius plot shows linear regression with very high coefficients of determination. The largest slope, and consequently the highest activation energy, was observed for the reaction rate constant k_1, which describes the initial addition to form OME_2 from DMM. With increasing chain length the activation energy decreases significantly from 99 to about 82 kJ mol^{-1}. From a chain length of n=4, the required activation energy reaches a plateau and remains rather constant for a further increasing OME chain. The last determined value, k_5, deviates slightly from this trend. This may be due to the small amount of OME_6 formed during the temperature-dependent experiments and hence, being an artefact within the overall experimental error. A similar behaviour is found for the pre-exponential factor with a decreasing order of magnitude with increasing OME chain length. The observed behaviour fits to the explanations of the rate limiting step for the formation reaction of OME_2 und OME_3 due to the limited FA availability. The higher activation energy in this case is based on the activation barrier of the trioxane decomposition as the rate limiting step. As for the rather constant rate constants for the formation of higher OME for which the limitation by FA can be excluded the activation barrier is also rather constant and represents the actual activation barrier of the chain growth step. Compared to conventional catalysts the higher activity of the heteropoly acid due to a lower activation barrier is obvious. E.g., Amberlyst-15 showed an activation energy of 112 kJ mol^{-1}.[33] Lower activation energies are only reported for molecular catalysts dissolved in the liquid phase such as a sulfonic acid-functionalized ionic liquid as catalyst.[34]

Conclusions

In this work we showed for the first time the superior performance of phosphotungstic acid as catalyst for the formation of oxymethylene ethers from methylal and trioxane. A screening of acidic catalysts and suitable window of reaction conditions proved the significantly increased activity of the heteropoly acid compared to conventional solid acids. The selectivity for the short chain oligomers, especially to OME_{3-5} which are the most suitable fuel additive fraction, can be controlled well by adjusting the reaction parameters. A detailed kinetic investigation for the heteropoly acids was carried out. By applying a suitable model for the reaction network the experimental data can be described very well. It was shown that the backward reactions are orders of magnitudes smaller than the forward reactions and hence, the reversibility of the reaction does not facilitate any equilibrium limitations. The kinetic parameters activation energy and pre-exponential factor prove the significantly higher catalytic activity compared to conventional solid acid catalysts. Also, it was shown that for the initial two OME formation reactions the FA availability from the trioxane decomposition is the rate limiting step. Overall, it is demonstrated that heteropoly acids might be a very good catalyst choice for an efficient and well-controllable production of short chain OME as synthetic fuel additives. Considering the solubility of phosphotungstic acid in water, alcohols and ethers a minor solubility in the OME mixture was observed although no quantitative dissolution occurred. Nevertheless, for further reaction optimization well-known routes for the immobilization of heteropoly acids will have to be applied to ensure a heterogeneous behaviour of the catalyst and avoid leaching upon continuous processing.

Experimental

Materials and methods

Methylal (Grignard reaction grade, ≥99 %), trioxane (≥99 %), tungstic acid (99 %) and phosphotungstic acid (reagent grade) were purchased from Sigma Aldrich. Tungsten oxide was ordered from Alfa Aesar. Puralox powders are from Sasol and Purolite CT175DR from Purolite. ZSM-5 was obtained from BASF, H-BEA 25 from Clariant. Phosphotungstic acid was dried overnight in a vacuum oven at 60 °C to remove the crystallization water[35] and stored in an desiccator before use.

Reactions in steel autoclave. A stainless steel pressure reactor (autoclave) with electrical heating and a reactor volume of 300 mL is used. 2.4 eq. (86 g, 1.13 mol) of DMM, 1 eq. (43 g, 0.47 mol) of trioxane and 5 wt-% (6.79 g) of the respective catalyst is filled into the reactor before closing and heating up. In order to remove dissolved gases from the solution, the reactor is filled with argon by stirring at 1000 rpm up to a pressure of 10 bar. After equilibration the reactor pressure is reduced to 2 bar. This procedure is repeated three times. The reactor was heated up to 60 °C. Due to the vapour pressure an autogenous pressure of about 3.1 bar is obtained. The temperature of the solution is controlled by a digital thermometer in the solution. Samples were taken by a sampling valve with a dip tube in the reaction solution.

Reactions in glass reactor. In a 100 mL three neck round bottom flask with reflux condenser and alcohol thermometer, 50 mL of methylal and the DTR corresponding amount of trioxane are mixed. The solution was heated with an oil bath to the desired temperature. If the temperature is constant for 10 minutes, 0.1102 g of catalyst are added to the stirred solution via a funnel. Samples were taken by a neck of the flask in regular time intervals.

Gas Chromatography. To determine the composition of the reaction mixtures gas chromatography with an Optima WAxPlus column and a flame ionization detector (FID) is used. The calibration was carried out by injecting the pure components including OME_n up to chain length n=4 dissolved in toluene with 1,4-dioxane as an internal standard. A five-point determination was carried out. For the calibration for a higher chain length, the ratio between calibration factor to molar mass from OME_1 to OME_4 are extrapolated linearly up to OME_8. The accuracy of the mass fractions is about ±0.1 mg absolute deviation; corresponding to an experimental error of 3.3 %. This was verified by the overall found mass via calculated GC areas and the difference to the weight of the sample of the reaction solution.

Conflicts of interest

There are no conflicts to declare

Acknowledgements

We gratefully acknowledge financial support by the Federal Ministry of Education and Research (BMBF), Grant No. 031B0680.

References

1. J. C. Serrano-Ruiz and J. A. Dumesic, *Energy Environ. Sci.*, 2011, **4**, 83-99.
2. A. Sternberg and A. Bardow, *Energy Environ. Sci.*, 2015, **8**, 389-400.
3. C. J. Baranowski, A. M. Bahmanpour and O. Kröcher, *Appl. Catal. B: Environ.*, 2017, **217**, 407-420.
4. S. Deutz, D. Bongartz, B. Heuser, A. Kätelhön, L. Schulze Langenhorst, A. Omari, M. Walters, J. Klankermayer, W. Leitner, A. Mitsos, S. Pischinger and A. Bardow, *Energy Environ. Sci.*, 2018, **11**, 331-343.
5. J. Burger, M. Siegert, E. Ströfer and H. Hasse, *Fuel*, 2010, **89**, 3315-3319.
6. C. H. Gierlich, K. Beydoun, J. Klankermayer and R. Palkovits, *Chem. Ing. Tech.*, 2020, **92**, 116-124.
7. K. Hackbarth, P. Haltenort, U. Arnold and J. Sauer, *Chem. Ing. Tech.*, 2018, **90**, 1520-1528.
8. B. Lumpp, D. Rothe, C. Pastötter, R. Lämmermann and E. Jacob, *MTZ worldwide eMagazine*, 2011, **72**, 34-38.
9. R. Sun, I. Delidovich and R. Palkovits, *ACS Catalysis*, 2019, **9**, 1298-1318.
10. L. Lautenschütz, D. Oestreich, P. Seidenspinner, U. Arnold, E. Dinjus and J. Sauer, *Fuel*, 2016, **173**, 129-137.
11. K. Thenert, K. Beydoun, J. Wiesenthal, W. Leitner and J. Klankermayer, *Angew. Chem. Int. Ed.*, 2016, **55**, 12266-12269.
12. B. G. Schieweck and J. Klankermayer, *Angew. Chem. Int. Ed.*, 2017, **56**, 10854-10857.
13. A. M. Bahmanpour, A. Hoadley, S. H. Mushrif and A. Tanksale, *ACS Sustainable Chem. Eng.*, 2016, **4**, 3970-3977.
14. D. Deutsch, D. Oestreich, L. Lautenschütz, P. Haltenort, U. Arnold and J. Sauer, *Chem. Ing. Tech.*, 2017, **89**, 486-489.
15. N. Schmitz, F. Homber, J. Berje, J. Burger and H. Hasse, *Ind. Eng. Chem. Res.*, 2015, **54**, 6409-6417.
16. J. Burger, E. Ströfer and H. Hasse, *Ind. Eng. Chem. Res.*, 2012, **51**, 12751-12761.
17. N. Schmitz, J. Burger and H. Hasse, *Ind. Eng. Chem. Res.*, 2015, **54**, 12553-12560.
18. C. J. Baranowski, A. M. Bahmanpour, F. Héroguel, J. S. Luterbacher and O. Kröcher, *Catal. Sci. Technol.*, 2019, **9**, 366-376.
19. D. Deutsch, D. Oestreich, L. Lautenschütz, P. Haltenort, U. Arnold and J. Sauer, *Chem. Ing. Tec.*, 2017, **89**, 486-489.
20. Y. Zheng, Q. Tang, T. Wang and J. Wang, *Chem. Eng. Sci.*, 2015, **134**, 758-766.
21. A. Fink, C. H. Gierlich, I. Delidovich and R. Palkovits, *ChemCatChem*, 2020, **12**, 5710-5719.
22. J. Burger, E. Ströfer and H. Hasse, *Ind. Eng. Chem. Res.*, 2012, **51**, 12751-12761.
23. L. Wang, W.-T. Wu, T. Chen, Q. Chen and M.-Y. He, *Chem. Eng. Com.*, 2014, **201**, 709-717.
24. L. Lautenschütz, D. Oestreich, P. Haltenort, U. Arnold, E. Dinjus and J. Sauer, *Fuel Processing Technology*, 2017, **165**, 27-33.
25. I. V. Kozhevnikov, *Chem. Rev.*, 1998, **98**, 171-198.
26. H. N. Miras, J. Yan, D.-L. Long and L. Cronin, *Chem. Soc. Rev.*, 2012, **41**, 7403-7430.
27. DE102005027702 (A1), 2006.
28. DE102017201691 (A1), 2017.
29. DE102019101927 (A1), 2019.
30. PRESTO KINETICS, https://cit-wulkow.de).
31. J. F. Walker and A. F. Chadwick, *Ind. Eng. Chem.*, 1947, **39**, 974-977.
32. V. A. Giefer and W. Kern, *Die Makromolekulare Chemie*, 1964, **74**, 39-45.
33. R. Peláez, P. Marín and S. Ordónez, *Chem. Eng. J.*, 2020, **396**, 125305.
34. D. Wang, F. Zhao, G. Zhu and C. Xia, *Chem. Eng. J.*, 2018, **334**, 2616-2624.
35. C. Pazé, S. Bordiga and A. Zecchina, *Langmuir*, 2000, **16**, 8139-8144.